



## Experimental challenges and prospects for BSM discovery in heavy-quark pair production above the Z-pole energy

A. Irlés\*, J.P. Márquez\*, A. Saibel\*

\* *IFIC, Universitat de València and CSIC, C./ Catedrático José Beltrán 2, E-46980 Paterna, Spain*

The precise reconstruction of the  $AFB_q$  with  $q$  being  $c$ - or  $b$ -quarks poses several challenges. The experimental input is based on detailed simulations of the ILD at ILC with center-of-mass energies of 250 and 500 GeV and extrapolated to 1000 GeV. This study highlights the importance of precise vertexing, high acceptance forward tracker detectors, efficient charged-hadron particle identification capabilities, high-energy reach and longitudinal beams polarization for the deepest and most comprehensive scrutiny of the SM and beyond in heavy-quark pair production.

The search for new physics at the LHC and future electron-positron colliders requires a global approach that includes a detailed study of the heavy-quark production above the Z-pole energy. New resonances can be probed at these energies with precise measurements of  $EW$ -type observables. In Ref. [1] and here, the prospects to discover benchmark GHU models [2–10] using forward-backwards asymmetry,  $AFB_q$ , and observables at the ILC are discussed. In a nutshell, these benchmark models are characterized by:

The  $A$  models ( $A_1$  and  $A_2$ ) and  $B$  models ( $B_j^\pm$  with  $j = 1, 2, 3$  indicating the sign of the lepton bulk masses) as described in Ref. [1], are adopted as benchmark points:

$$A_1 : \rightarrow m_{Z'} = 7.19 \text{ TeV}; A_2 : \rightarrow m_{Z'} = 8.52 \text{ TeV},$$

$$B_1^\pm : \rightarrow m_{Z'} = 10.2 \text{ TeV}; B_2^\pm \rightarrow m_{Z'} = 14.9 \text{ TeV}; B_3^\pm \rightarrow m_{Z'} = 19.6 \text{ TeV};$$

where  $Z'$  is the first KK  $Z$  boson. The masses of the first KK  $\gamma$  and  $Z_R$  bosons are similar to those of the first KK  $Z$  boson.

The precise reconstruction of the  $AFB_q$  with  $q$  being  $c$ - or  $b$ -quarks poses several challenges. The experimental input is based on detailed simulations of the ILD at center-of-mass energies of 250 and 500 GeV and extrapolated to 1000 GeV. The fully differential cross-section  $d\sigma/d\cos\theta$  reconstruction is studied. With the current layout of the ILD detector for ILC, the  $d\sigma/d\cos\theta$  can be well reconstructed, with homogeneous reconstruction efficiency in  $-0.9 < \cos\theta < 0.9$ . At higher angles, the vertex reconstruction efficiency starts to drop and large corrections fully dependent on Monte Carlo simulations and detector modelling need to be applied. Novel geometries or reconstruction algorithms should be considered.

The studies conducted at ILC250 and ILC500 have been completed, demonstrating that a high level of statistical precision is attainable. In Ref. [1], state-of-the-art LCFIPlus, which relies on *traditional* Machine Learning (BDT) algorithms, was utilized for flavour tagging. Additionally, the ILD offers the crucial capability of providing charged-kaon identification across a broad momentum spectrum using TPC information.

Experimental systematic uncertainties were found to be sub-dominant, attributed to a) the anticipated excellent vertexing and flavour-tagging capabilities at the ILC, b) the use of fully differential measurements, and c) employing double-tagging and double-charge measurements that minimize reliance on Monte Carlo tools to address modelling uncertainties, such as hadronization uncertainties. Accurate estimation of the uncertainties in tagging efficiencies (and mis-tagging rates) can only be achieved at a high level of precision if perfect detector modelling and Monte Carlo tools with exceptional parton-shower and hadronization descriptions are available. The practical alternative would be to employ data-driven techniques like double-tagging and double-charge measurement methods.

Figure 1 shows the expected uncertainties for the reconstruction of  $AFB_b$  and  $AFB_c$  using full-simulation of signal and background events in the ILD model of [11], plus two additional scenarios on the detector model or reconstruction tools. The study was done for the available samples of ILC250 and ILC500.

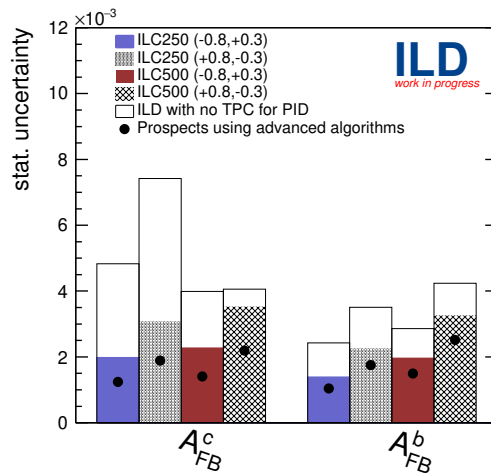


Figure 1: Estimated statistical uncertainties on  $AFB_c$  and  $AFB_b$  using ILD full simulation and reconstruction at ILC250 and ILC500. Two alternative scenarios of ILD model and reconstruction are shown.

Figure 2 discusses the sensitivity to BSM models in different possible running scenarios of ILC. The results for ILC1000 have been extrapolated from the studies at 500 GeV. The ILC250 case has also been compared with an ILC250 without beam polarization. For the latter case, it shows that at least a factor of two of integrated luminosity is required to get similar prospects.

Finally, three scenarios of different reconstruction capabilities are compared in Figures 1 and 2: a detector without charged-hadron particle identification capabilities (*i.e.*, a hypothetical version of ILD without a TPC-based central tracker); a state-of-the-art ILD detector with reconstruction tools described in Ref. [11] and cluster counting for the charged-hadron particle identification using the TPC; an improved scenario after applying modern reconstruction techniques based on advanced Artificial Intelligence models. These latter prospects are obtained by simply extrapolating from the *baseline* case considering the expected improvements on flavour-tagging discussed in Ref. [12]. The same improvement is assumed for the charged-hadron particle identification. It is important to remark the importance of charged-hadron particle identification (PID) specially for the c-quark case at ILC250, although the benchmark models discussed here show small sensitivity for ILC250. Detailed studies using full-simulation should be conducted to confirm these expectations.

This study highlights the importance of precise vertexing, high acceptance forward tracker detectors, efficient charged-hadron particle identification capabilities, high-energy reach and longitudinal beams polarization for the deepest and most comprehensive scrutiny of the SM and beyond.

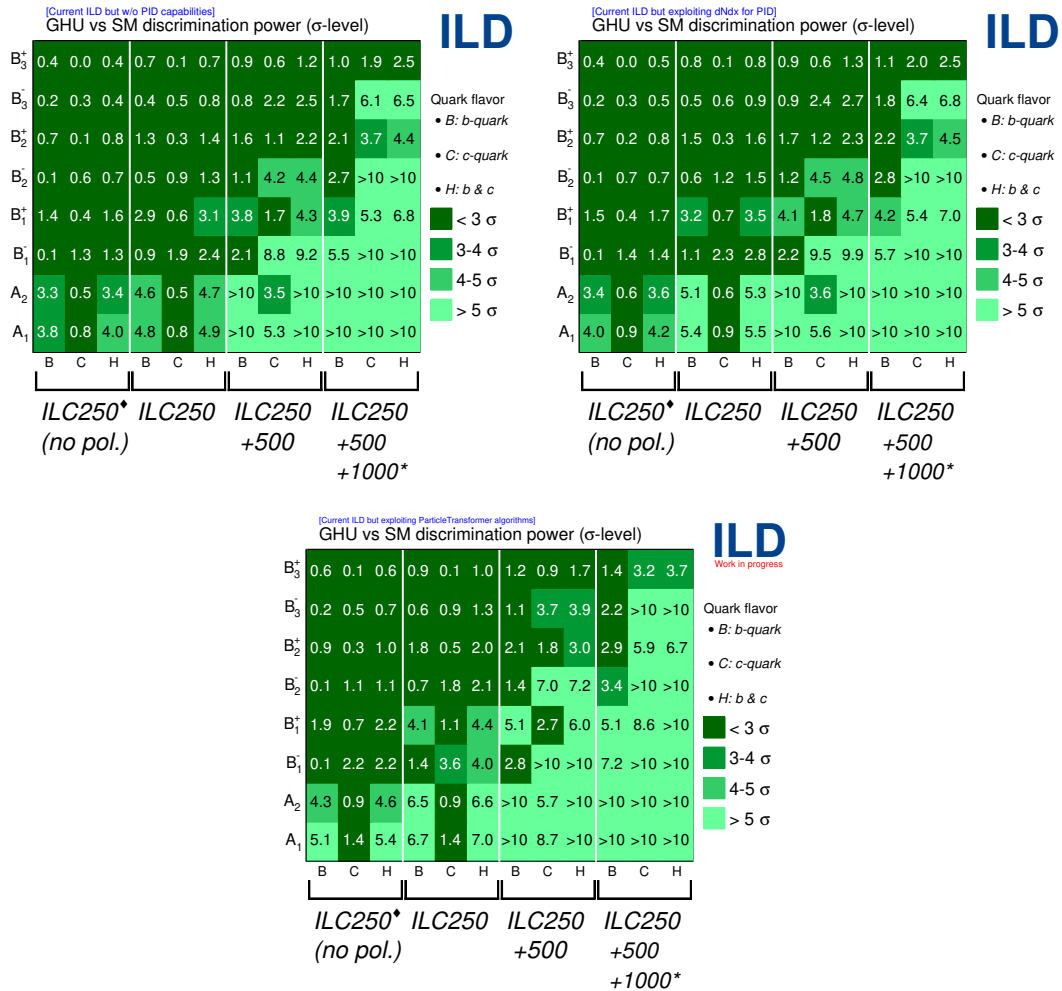


Figure 2: Statistical discrimination power between the GHU models described in the text and the SM. Different running scenarios of ILC are compared: ILC250(*no pol.*) (hypothetical case with no beam polarization and  $2000 \text{ fb}^{-1}$  of integrated luminosity), ILC250 ( $2000 \text{ fb}^{-1}$ ), ILC500 ( $4000 \text{ fb}^{-1}$ ), and ILC1000\* ( $8000 \text{ fb}^{-1}$ , not using full simulation studies but extrapolations of uncertainties from ILC500).

## 1 References

- [1] A. Irlles et al., *Probing gauge-Higgs unification models at the ILC with quark–antiquark forward–backward asymmetry at center-of-mass energies above the Z mass*, Eur. Phys. J. C **84** (2024) 537, DOI: [10.1140/epjc/s10052-024-12918-z](https://doi.org/10.1140/epjc/s10052-024-12918-z), arXiv: [2403.09144](https://arxiv.org/abs/2403.09144) [hep-ph].
- [2] K. Agashe, R. Contino, A. Pomarol, *The Minimal composite Higgs model*, Nucl. Phys. B **719** (2005) 165, DOI: [10.1016/j.nuclphysb.2005.04.035](https://doi.org/10.1016/j.nuclphysb.2005.04.035), arXiv: [hep-ph/0412089](https://arxiv.org/abs/hep-ph/0412089).
- [3] A. D. Medina, N. R. Shah, C. E. M. Wagner, *Gauge-Higgs Unification and Radiative Electroweak Symmetry Breaking in Warped Extra Dimensions*, Phys. Rev. D **76** (2007) 095010, DOI: [10.1103/PhysRevD.76.095010](https://doi.org/10.1103/PhysRevD.76.095010), arXiv: [0706.1281](https://arxiv.org/abs/0706.1281) [hep-ph].
- [4] Y. Hosotani et al., *Dynamical Electroweak Symmetry Breaking in  $SO(5) \times U(1)$  Gauge-Higgs Unification with Top and Bottom Quarks*, Phys. Rev. D **78** (2008), [Erratum: Phys.Rev.D 79, 079902 (2009)] 096002, DOI: [10.1103/PhysRevD.78.096002](https://doi.org/10.1103/PhysRevD.78.096002), arXiv: [0806.0480](https://arxiv.org/abs/0806.0480) [hep-ph].
- [5] S. Funatsu et al., *LHC signals of the  $SO(5) \times U(1)$  gauge-Higgs unification*, Phys. Rev. D **89** (2014) 095019, DOI: [10.1103/PhysRevD.89.095019](https://doi.org/10.1103/PhysRevD.89.095019), arXiv: [1404.2748](https://arxiv.org/abs/1404.2748) [hep-ph].
- [6] S. Funatsu et al., *GUT inspired  $SO(5) \times U(1) \times SU(3)$  gauge-Higgs unification*, Phys. Rev. D **99** (2019) 095010, DOI: [10.1103/PhysRevD.99.095010](https://doi.org/10.1103/PhysRevD.99.095010), arXiv: [1902.01603](https://arxiv.org/abs/1902.01603) [hep-ph].
- [7] S. Funatsu et al., *Fermion pair production at  $e^-e^+$  linear collider experiments in GUT inspired gauge-Higgs unification*, Phys. Rev. D **102** (2020) 015029, DOI: [10.1103/PhysRevD.102.015029](https://doi.org/10.1103/PhysRevD.102.015029), arXiv: [2006.02157](https://arxiv.org/abs/2006.02157) [hep-ph].
- [8] S. Funatsu et al., *Signals of  $W'$  and  $Z'$  bosons at the LHC in the  $SU(3) \times SO(5) \times U(1)$  gauge-Higgs unification*, Phys. Rev. D **105** (2022) 055015, DOI: [10.1103/PhysRevD.105.055015](https://doi.org/10.1103/PhysRevD.105.055015), arXiv: [2111.05624](https://arxiv.org/abs/2111.05624) [hep-ph].
- [9] S. Funatsu et al., *Single Higgs boson production at electron-positron colliders in gauge-Higgs unification*, Phys. Rev. D **107** (2023) 075030, DOI: [10.1103/PhysRevD.107.075030](https://doi.org/10.1103/PhysRevD.107.075030), arXiv: [2301.07833](https://arxiv.org/abs/2301.07833) [hep-ph].
- [10] N. Yamatsu et al., *W and Z boson pair production at electron-positron colliders in gauge-Higgs unification*, Phys. Rev. D **108** (2023) 115014, DOI: [10.1103/PhysRevD.108.115014](https://doi.org/10.1103/PhysRevD.108.115014), arXiv: [2309.01132](https://arxiv.org/abs/2309.01132) [hep-ph].
- [11] H. Abramowicz et al., ILD Concept Group, *International Large Detector: Interim Design Report (2020)*, arXiv: [2003.01116](https://arxiv.org/abs/2003.01116) [physics.ins-det].
- [12] R. Tagami, T. Suehara, M. Ishino, *Application of Particle Transformer to quark flavor tagging in the ILC project (2024)*, arXiv: [2410.11322](https://arxiv.org/abs/2410.11322) [hep-ex].